iScience

CellPress
OPEN ACCESS

Article

Top-down reconfiguration of SMA cortical connectivity during action preparation

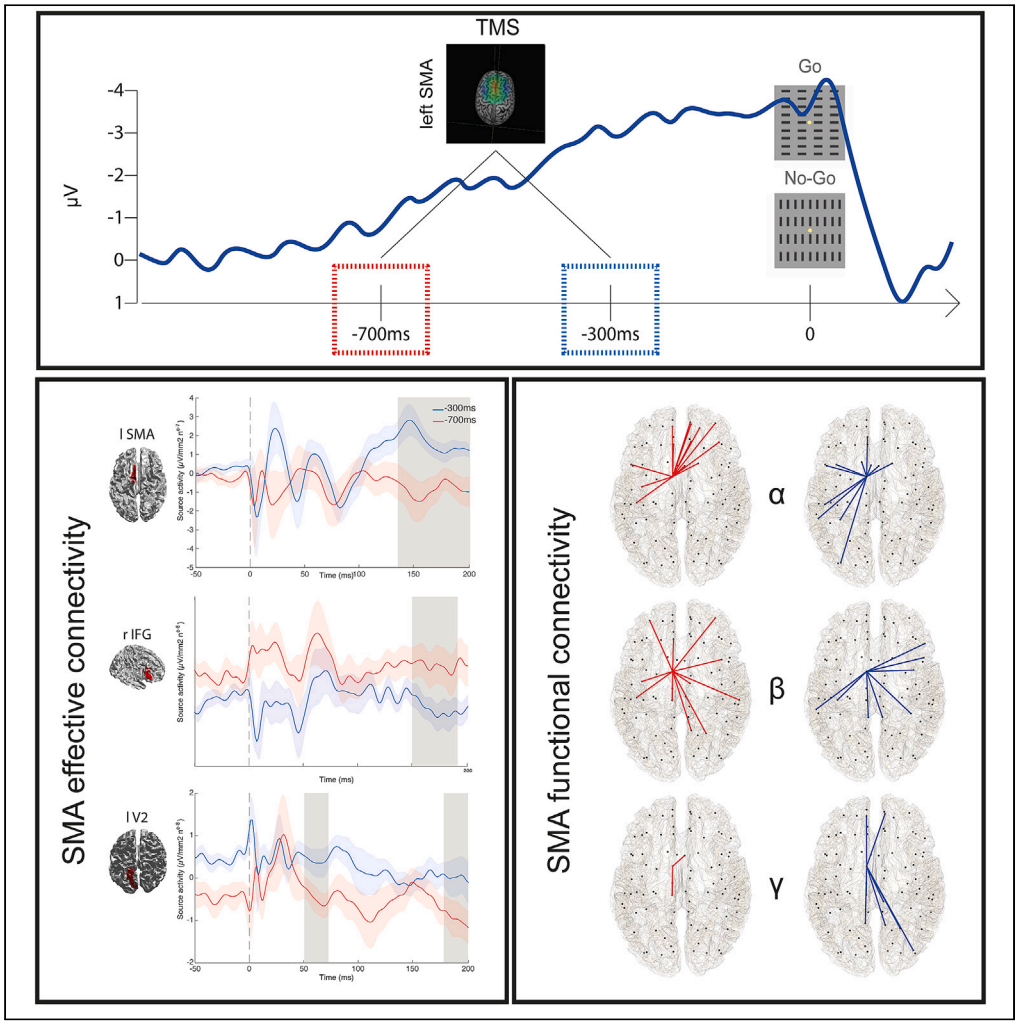

Valentina Bianco, Eleonora Arrigoni, Francesco Di Russo, Leonor Josefina Romero Lauro, Alberto Pisoni

e.arrigoni6@campus.unimib.it (E.A.)
alberto.pisoni@unimib.it (A.P.)

Highlights

We explored cortical excitability and connectivity of the SMA during the BP

The BP reflects the activity of distributed networks extending beyond SMA

SMA effective connectivity with prefrontal and occipital regions changes over time

SMA α, β, and γ functional connectivity change as action preparation unfolds

Bianco et al., iScience *26*, 107430
August 18, 2023
https://doi.org/10.1016/j.isci.2023.107430

iScience

CellPress
OPEN ACCESS

Article

Top-down reconfiguration of SMA cortical connectivity during action preparation

Valentina Bianco,[1,6] Eleonora Arrigoni,[2,6,*] Francesco Di Russo,[3] Leonor Josefina Romero Lauro,[4,5] and Alberto Pisoni[4,5,7,*]

SUMMARY

The Bereitschaftspotential (BP), a scalp potential recorded in humans during action preparation, is characterized by a slow amplitude increase over fronto-central regions as action execution approaches. We recorded TMS evoked-potentials (TEP) stimulating the supplementary motor area (SMA) at different time-points during a Go/No-Go task to assess whether and how cortical excitability and connectivity of this region change as the BP increases. When approaching BP peak, left SMA reactivity resulted greater. Concurrently, its effective connectivity increased with the left occipital areas, while it decreased with the right inferior frontal gyrus, indicating a fast reconfiguration of cortical networks during the preparation of the forthcoming action. Functional connectivity patterns supported these findings, suggesting a critical role of frequency-specific inter-areal interactions in implementing top-down mechanisms in the sensorimotor system prior to action. These findings reveal that BP time-course reflects quantitative and qualitative changes in SMA communication patterns that shape mechanisms involved in motor readiness.

INTRODUCTION

Action preparation is characterized by multiple stages of processing. Multimodal representations about the external world and the internal states are processed together to guide motor behavior, biasing the activity of the sensorimotor system to ensure the selection and execution of a motor plan at the most appropriate moment in time.[1,2] In the early stages of action preparation, slow cortical potentials can be recorded with electroencephalography (EEG), reflecting complex neurophysiological events related to motor anticipation and proactive control of movement.[3] Pre-movement potentials have been extensively used to understand the processes taking place before movement generation both in healthy participants and clinical conditions affected by movement disorders.[4,5] In particular, the Bereitschaftspotential (BP) is a slow negative cortical potential preceding the onset of voluntary movement, reflecting an increase in cortical excitability of the premotor regions during motor preparation.[5] Based on its spatiotemporal characteristics, BP can be divided into two phases: the earliest phase starts approximately 1–2 s before the voluntary movement and slowly rises over fronto-central regions with a symmetrical distribution; during the later phase, the potential suddenly increases its gradient around 500 ms before movement onset, displaying a steeper negative slope (i.e., late BP) and reaching a maximal amplitude (i.e., motor potential) over the contralateral central area.[5]

Converging evidence suggests that pre-movement negativity may have different functional meanings, reflecting specific processes taking place during the early stages of motor preparation: BP amplitude is influenced by basic movement features (e.g., force, and speed), complexity, selection, effort, intentionality, and also higher cognitive aspects, such as gesture meaning, emotional valence, contextual aspects, and consequences of the action itself.[3,5] However, it is unknown if this event merely relates to the increased recruitment of the motor network over the time-course of action preparation, or if a functional reorganization occurs beyond the motor and premotor regions as action execution, and thus the late phase of the BP, approaches. As a matter of fact, beyond premotor areas, a distributed network of cortical and subcortical regions also plays a crucial role in regulating different stages of action preparation, including decision-making processes and other computations related to the prediction of forthcoming events taking place in the surrounding environment.[3]

[1]Department of Brain and Behavioral Sciences, University of Pavia, 27100 Pavia, Italy

[2]PhD Program in Neuroscience, School of Medicine and Surgery, University of Milano-Bicocca, Via Cadore 48, 20900 Monza, Italy

[3]Department of Movement, Human and Health Sciences, University of Rome "Foro Italico", Piazza Lauro De Bosis, 15, 00135 Rome, Italy

[4]Department of Psychology, University of Milano-Bicocca, P.zza dell'Ateneo Nuovo 1, 20126 Milan, Italy

[5]NeuroMi, Milan Centre for Neuroscience, Milan, Italy

[6]These authors contributed equally

[7]Lead contact

*Correspondence: e.arrigoni6@campus.unimib.it (E.A.), alberto.pisoni@unimib.it (A.P.)

https://doi.org/10.1016/j.isci.2023.107430

Neuroimaging and brain stimulation studies[6–12] provided useful information on the main generators of the BP: the initial segment of the early BP is assumed to be linked to the bilateral activation of the supplementary motor area (SMA) and the cingulate motor area (CMA), thereafter the progressive increase in the potential's amplitude likely reflects the additional involvement of the lateral premotor and, in the late phase, of primary motor areas, thus possibly reflecting the increasing interactions between the fronto-medial structures and the sensorimotor regions.[13–15] However, it is unclear whether the BP time-course simply reflects the activation state of premotor and motor regions before movement, or a functional reorganization occurs beyond the motor system, involving a proactive change in inter-areal communication between the main generator of such premotor Event Related Potential (ERP; i.e., the SMA) and other nodes within the action preparation network in view of the forthcoming action.

The present study aimed at exploring the changes in global cortical dynamics underlying the BP spatiotemporal evolution using an integrated transcranial magnetic stimulation (TMS) and EEG system.

TMS-EEG co-registration allows to probe real-time cortical reactivity through the analysis of TMS-evoked potentials (TEPs). TEPs are considered a reliable measure of cortical excitability, thus indexing the state of activation of the stimulated area.[16,17] Furthermore, TEPs analysis allows to observe the spatiotemporal propagation of the activity induced by TMS spreading in remote regions throughout functionally relevant connections, providing information about effective cortical connectivity.[18] Finally, the analysis of TEP's oscillatory features can inform about inter-regional functional connectivity, potentially tapping at modulations of qualitative components of inter-areal communication.[19]

In this study, healthy participants performed an equiprobable, visuomotor Go/No-Go task[20] across four TMS-EEG recordings in which left SMA and a control region (i.e., left extrastriate area) were stimulated. The task was used because has been widely used in ERP literature, but also because this task is complex enough to involve, in addition to the SMA, prefrontal and sensory areas during action preparation stages (for normative ERP data of this task see[20]). TMS pulse occurred at two different times before stimulus presentation, in correspondence to the beginning (i.e., −700 ms) and the peak (i.e., −300 ms) of the BP, while TEPs were recorded from 60 scalp electrodes (see Figure 1A for the experimental timeline). This set-up allowed to explore the differences in cortical excitability of the SMA during the BP time-course by comparing at the source level TEPs at the two stimulus onset asynchronies (SOAs). At the same time, source-level effective and functional connectivity analysis complemented this knowledge by assessing the networks in which the SMA was involved during different time-points of action preparation, hence allowing to explore the functional meaning of the neurophysiological activity recorded before action onset.

RESULTS

Behavioral results

Participants' behavioral performance was in line with the literature using the same Go/No-Go paradigm with a comparable inter-stimulus interval,[21] and, as expected, showed no difference across No-TMS, SMA, and extrastriate stimulation recordings (all ps > 0.05, see Figure 1C and supplemental information) for both reaction times and accuracy scores. The high accuracy in performing the Go/No-Go task ensured the attention of the participants to the experimental procedures.

Pre-stimulus ERPs

The ERP waveforms and scalp topography related to the visual stimulus onset obtained in the No-TMS condition are shown in Figure 1B. The BP was detectable with an onset at −950 ms as a gentle increase just before the stimulus onset, reaching a maximal amplitude of 4 μV. In this period, the BP had a consistent scalp topography focusing on medial centro-parietal areas. This result confirms the presence of BP in the present paradigm.

Cortical reactivity and effective connectivity during BP time-course

First, TEPs grand average was computed at scalp-level for each condition (SMA SOA -300 ms, M = 112 trials, SD = 4.70; SMA SOA -700 ms, M = 111.89; SD = 4.70; extrastriate SOA -300 ms, M = 109, SD = 5.01; extrastriate SOA -700 ms, M = 107.73, SD = 5.37).

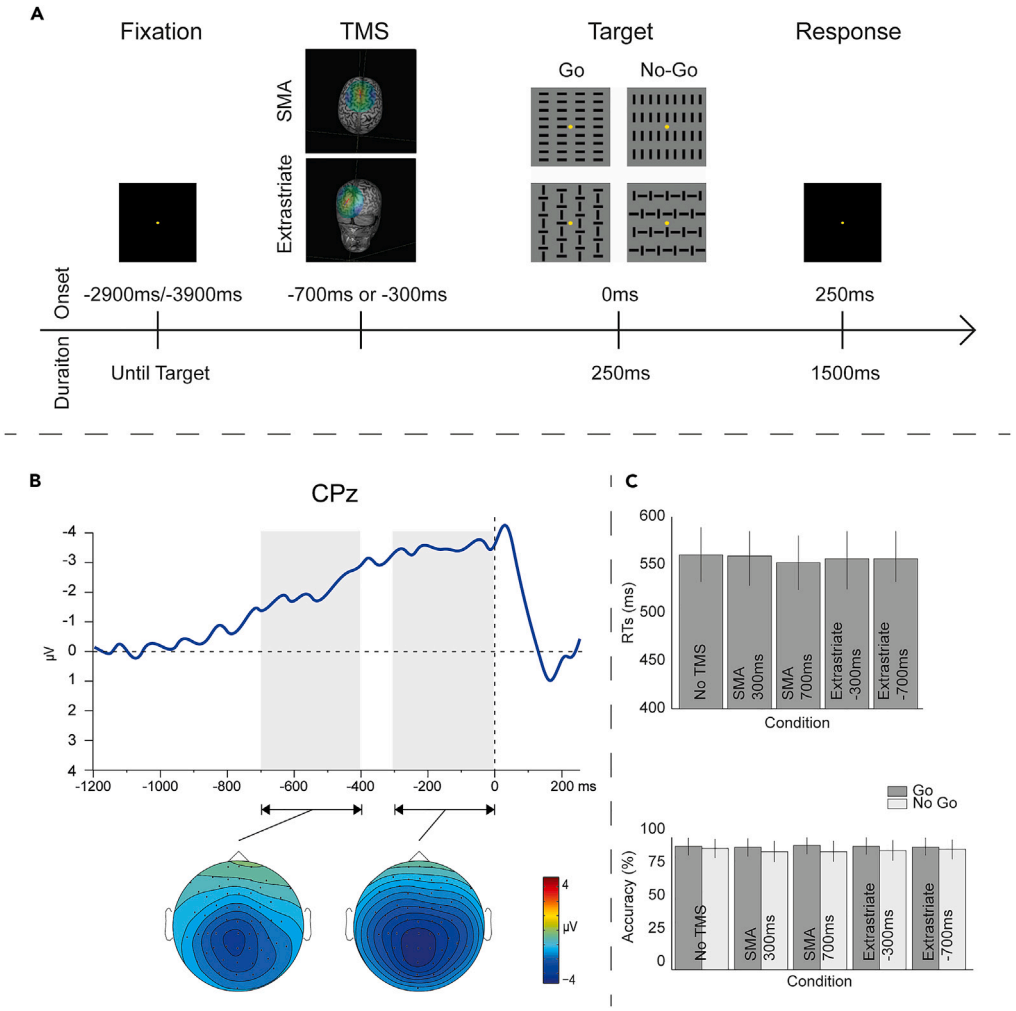

Figure 1. Paradigm description and quality check

(A) Experimental timeline. Trials started with a fixation screen, presented for a jittering interval between 2900 ms and 3900 ms. Within this interval, according to SOA condition, TMS was delivered −700 or −300 ms before Target onset on the left SMA or left extrastriate region, according to the experimental block. The Target appeared for 250 ms. Go and No-Go trials appeared with equal probability (p = 0.5), with each figure appearing 25% of the trials. Finally, a fixation screen was displayed to collect participants' response. In No TMS blocks, the experimental procedure remained the same but TMS was not delivered.

(B) Grand average of the pre-stimulus ERP in the No-TMS condition. BP time-course (upper row) and its scalp topography (bottom row, from −700 to −400 and from −300 to 0 ms) representing the early and late BP phases are displayed. The paradigm successfully elicited this pre-stimulus component.

(C) Behavioral results. Upper row: Mean RTs data in the five experimental conditions. Bottom Row: Mean Accuracy for Go and No-Go trials in the five experimental conditions. Error bars indicate ±1 SEM.

Figure 2 shows the butterfly plot of the grand average of the TEPs evoked by SMA stimulation at the −700 ms (upper row) and −300 ms (lower row) SOAs. For both the SOAs, the TMS pulse on SMA produced seven main components, peaking respectively around 5, 10, 20, 45, 65, 100, and 150 ms. At scalp level, the components did not show clear differences between the two SOAs (Figure 2). Concerning the control occipital stimulation, five main components were observed, reaching their peaks respectively around 5, 10, 30, 80, and 150 ms. All the components were spatially distributed over the stimulated area (left parieto-occipital region), with no appreciable difference between SOAs (see supplemental information).

For both stimulation targets (i.e., left SMA and left extrastriate), we compared the amplitude of cortical activation triggered by TMS between the two SOAs (i.e., −700 ms vs. −300 ms) within cortical parcels

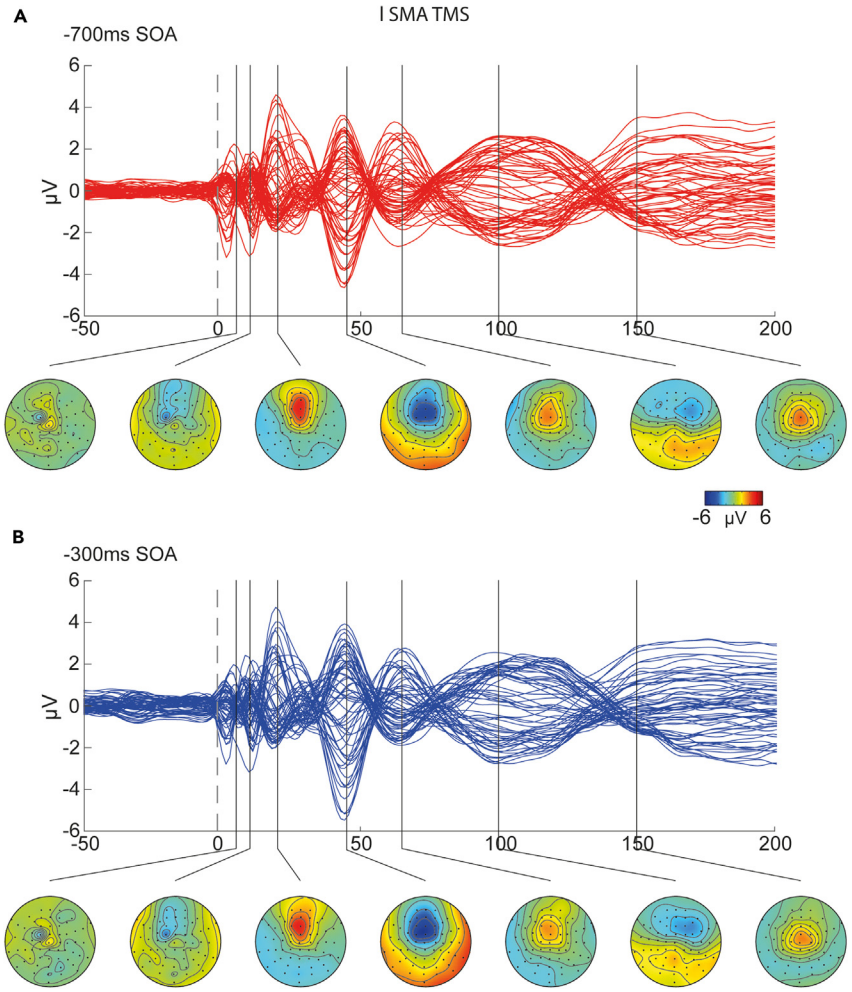

Figure 2. Grand average results from sensor-space TEPs analyses after SMA stimulation

(A) Butterfly plots of TEPs recorded in −700 ms SOA trials (red lines).

(B) Butterfly plots of TEPs in the −300 ms SOA condition (blue lines). Scalp topographies are plotted for the components peaking around 5 ms, 10 ms, 20 ms, 45 ms, 60 ms, 100 ms, and 150 ms for both SOAs conditions.

representing regions of interest (ROI) involved in the action preparation network: the left/right SMA, motor, premotor regions, secondary visual regions, and inferior frontal gyri. Specifically, to track changes in cortical excitability occurring during the BP time-course, we compared the amplitude of cortical activations at the two TMS SOAs (i.e., −700 ms vs. −300 ms) within each stimulation site condition (i.e., left SMA and left extrastriate).

The cluster-based comparison of source-level SMA TEPs within the parcel corresponding to the left SMA revealed a significant increase in amplitude (two positive clusters, ps < 0.05) in correspondence to the late (SOA -300 ms) compared to the early phase of the BP (SOA -700 ms) 140–175 ms and 179–200 ms (Figure 3). In order to assess inter-areal communication by quantifying TMS-evoked signal spread from the stimulated region to distant cortical nodes of the functional network involved in action preparation (i.e., effective connectivity,[22]), we further compared how SMA induced activity spread to the left/right motor and premotor cortices, as well as to the left/right superior occipital gyrus and the left/right inferior frontal gyrus (rIFG). We found a significant increase in cortical response within the occipital parcel (two positive clusters, ps < 0.05) in early (50–70 ms) and late components (180–200 ms) when TMS was triggered on SMA in correspondence to the late SOA. Conversely, we reported a significant reduction in TEPs amplitude within the rIFG in correspondence to the late SOA, as indexed by a significant

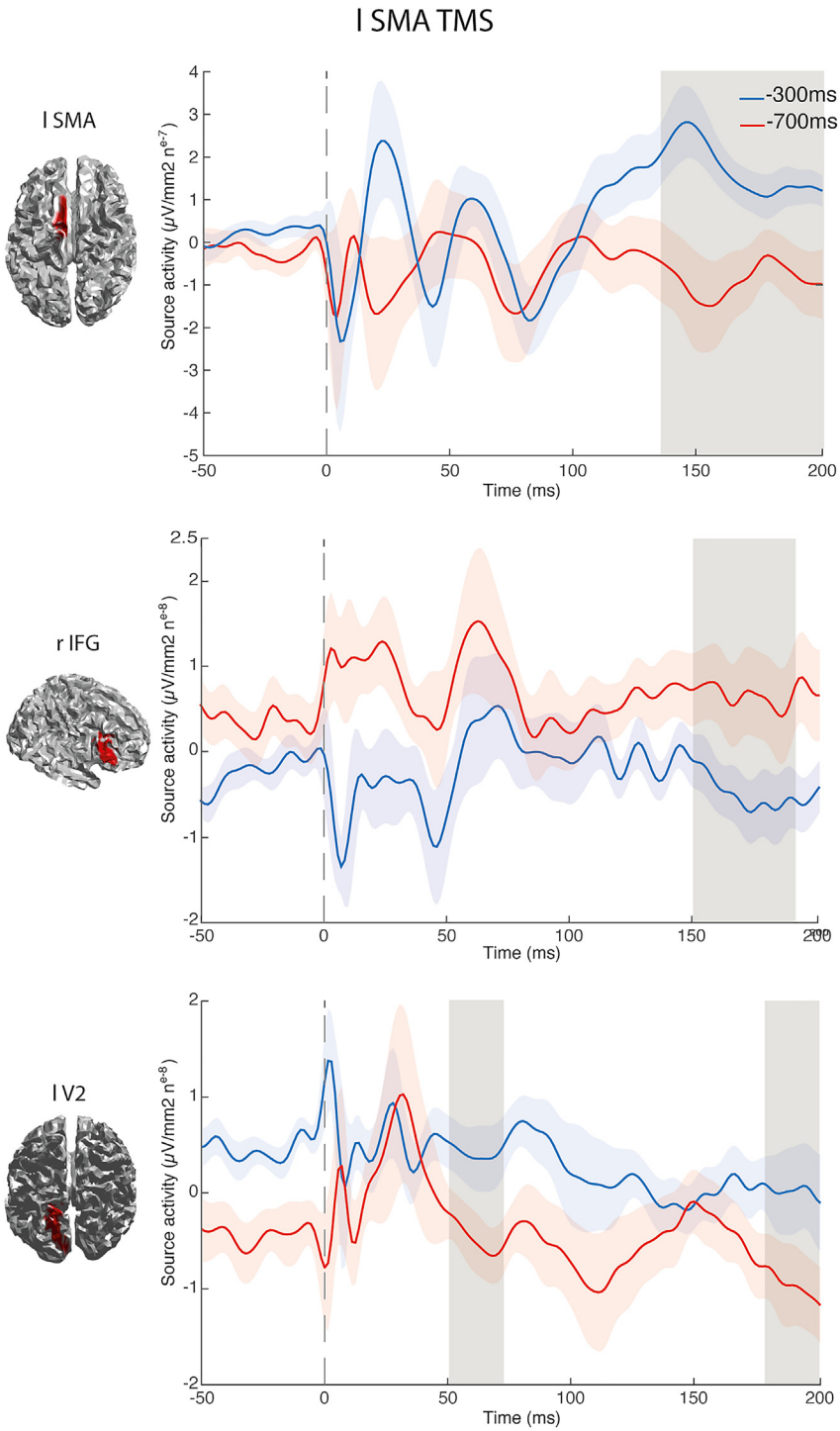

Figure 3. Grand average results from source-space TEPs analyses

ROI activity for local excitability (left SMA) and effective connectivity (right IFG and left extrastriate region, l V2) recorded in −700 ms SOA trials (red lines) and in the −300 ms SOA condition (blue lines) after left SMA stimulation. Red and blue shaded areas indicate ±1 SEM. Grey shaded areas indicate significant differences between SOAs.

negative cluster around 150–180 ms post TMS ($p < 0.05$; see Figure 3). To control for the specificity of the effects, we performed the same comparisons for the extrastriate region stimulation, where only a significant increase in cortical response within the left SMA in correspondence to the late SOA ($p = 0.04$,

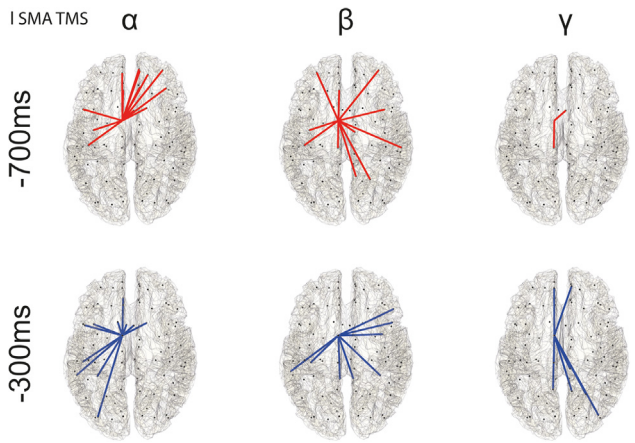

Figure 4. Source connectivity results

Plots for the alpha (8–12 Hz) beta (13–30 Hz) and low-gamma (31–40 Hz) bands during SMA TMS sessions for the −700 ms (upper row) and −300 ms (lower row) SOAs conditions are displayed. Black dots represent the centroids of the parcellated cortical regions. Connections start from the left SMA area. Labels of the connected regions are reported in Table S1. The connections represent wPLI values that survived statistical thresholding ($p < 0.01$) against surrogate data.

60–90 ms post TMS) was present (See supplemental information). No other cortical parcel showed significant differences in evoked activity between SOAs for both SMA and extrastriate TMS.

Left SMA functional connectivity during action preparation

To investigate functional connectivity changes during action preparation, we computed in the source-space the debiased weighted phase lag index (wPLI[23]) between each stimulation target (left SMA and left extrastriate) and the other cortical parcels within three frequency bands (i.e., alpha, 8–12 Hz; beta, 13–30 Hz; low gamma, 31–40 Hz). This analysis was also performed on a surrogate dataset created by shuffling the phase of the source reconstructed time series for each subject and each experimental condition. The resulting connectivity values have been corrected with a permutation approach against surrogate data obtained by shuffling the phase of the real datasets.

Figure 4 shows significant connections in the considered oscillatory bands between the left SMA and the other cortical regions (See Table S5 for cortical parcels labels; Occipital results are reported in the supplemental information).

At −700 ms SOA, TMS over the SMA revealed an alpha-band network, characterized by prominent connections with bilateral frontal and parietal parcels, encompassing the left precentral and postcentral gyri, the right superior and middle frontal areas, the orbital parts of the right prefrontal cortex, and the left inferior frontal gyrus. Moreover, SMA is connected to the bilateral anterior cingulate cortex. At −300 ms SOA, the SMA-related alpha-band network becomes more left-lateralized and posterior, comprising regions in the left temporal and occipital areas.

In the beta-band, during the early stage of the pre-stimulus period, the left SMA displayed bilateral connections with frontal, temporal, and parietal regions. We found significant interactions with the left precentral and postcentral gyri, the bilateral middle frontal areas, the anterior and mid-cingulate cortex, besides comprising connections with superior and medial portions of the parietal lobes, and the right superior and temporal cortices. Beta-band functional connectivity profile changed during the late stage of the pre-stimulus period, encompassing the right inferior frontal gyrus and the insula. Further, the left SMA increased its connectivity in the late time window with bilateral posterior portions of the cingulate cortex, parietal, and temporal regions.

Finally, TMS triggered at −700 ms SOA revealed the relative absence of low-gamma frequency interactions between the left SMA and other regions. At −300 ms SOA, new interactions arose between the left SMA and several regions in the frontal, parietal, and occipital lobe, encompassing the bilateral superior medial

frontal cortex, the right mid occipital gyrus, and bilateral superior, and medial regions within the parietal lobes, including the precuneus.

DISCUSSION

Our study investigated the activity and functional organization of motor networks during action preparation. The left SMA and the left extrastriate region were stimulated with single TMS pulses at different stages of action preparation, and scalp activity was recorded from a 60-channel compatible EEG. Cortical reactivity, signal spread, and functional connectivity were then analyzed in the source space to assess differences in early and late stages of the BP.

In line with previous literature, we confirmed the crucial role of the SMA in the generation of the BP: when TMS was delivered over the SMA in the late BP phase (i.e., SOA -300 ms), greater cortical activity was observed from the source reconstruction within the stimulated region. The reported difference in the magnitude of SMA responses to TMS between the two SOAs may be considered as a direct proof of the increased cortical excitability of the stimulated region during later stages of action preparation, in line with previous BP literature.[3,5] Interestingly, a similar result was found in SMA effective connectivity with the extrastriate regions, since occipital parcels' activity in response to SMA stimulation increased as the imperative signal approached. A similar result was found for extrastriate stimulation, with increased left SMA activity as the BP timecourse advances. Critically, as a control, occipital cortical reactivity did not change with BP timecourse.

The relevance of these results on signal amplitude increase is twofold: First, greater SMA activity as action approaches denotes a direct relationship between the BP and SMA activation. Second, the bidirectional increase in effective connectivity between SMA and extrastriate regions denotes a rise over time in communication between these two areas as action trigger approaches, likely driving visual readiness and a preactivation of the sensorimotor pathway crucial for task execution.

Conversely, cortical activity triggered by SMA stimulation decreased in correspondence of the rIFG as the visual stimulus approaches, indexing a reduction in effective connectivity between the two regions. In previous studies, pre-stimulus activity of the rIFG was related to proactive inhibitory control.[24] Proactive inhibition processes occur simultaneously to motor preparation and they both characterize the earlier stage of proactive control of motor behavior, preparing the motor system for action while preventing the implementation of a premature or inappropriate response. From an electrophysiological perspective, this proactive inhibition process has been identified by a negative component (i.e., pN, see[21]) that emerges about 1 s before the presentation of the imperative stimulus.[20] While the activation state of the SMA increases progressively as the action approaches, the rIFG activity rather decreases, until it disappears in the case of the presentation of a go signal, or remains sustained to prevent movement execution in case of no-go instruction.[21] The interplay between SMA and rIFG activity has been interpreted as a brake-accelerator system involved in pre-stimulus preparation and related to action anticipation.[21,25] Therefore, the observed reduction in effective connectivity from left SMA to rIFG might be related to the progressive release of the proactive inhibition during the pre-stimulus time-course.

Functional connectivity applied to TMS-EEG data allowed to highlight significant networks encompassing the left SMA and other regions that are known to be crucially involved in motor planning and action preparation. As the imperative stimulus approaches, SMA low-gamma band connectivity increased, which may support interareal communication which is crucial for local processing of multiple segregated inputs coming from different areas.[26–28] Gamma synchronization is indeed considered a key mechanism underlying precise, selective, and effective communication within activated networks, by orchestrating the activity of neuronal assemblies located in different brain regions but functionally related and engaged in the execution of a cognitive task.[29,30] Moreover, gamma synchronization has been related to a pro-kinetic role in the generation of voluntary movement (e.g.,[31–33]). Albeit almost absent in the early phase of BP, low-gamma band connections emerge in the later phase of pre-stimulus period, with bilateral interactions between the left SMA and other cortical regions belonging to the medial superior frontal, parietal and occipital cortices, particularly involved in the cognitive and perceptual aspects of action preparation and control.[34–37] Moreover, by the time stimulus presentation approaches, SMA-related gamma-band communication widens to posterior regions, which in turn are relevant for perceptual and attentional processing, suggesting an increase in the information flow between the frontal, executive brain areas, responsible for the selection and implementation of the motor output, and sensory brain areas, responsible for the processing and evaluation of the upcoming visual imperative stimulus.

Additionally, SMA-related alpha-band connectivity network changes from an anterior to posterior pattern as the BP reaches its peak, becoming more relevant on temporal and occipital regions as well. Alpha-band functional connectivity has been related to visual attention[38] and top-down neural networks responsible for attentional features crucial for task demands.[39,40] Previous evidence highlighted that regions in the dorsomedial frontal cortex could directly modulate alpha-band activity in the posterior visual areas, modulating visual stimuli sensitivity,[41] thus subserving top-down modulation of sensory activity.[42]

Qualitative changes were detected also in the SMA-related beta-band connectivity profile. We observed the emergence of beta-band interactions between the SMA and the rIFG during the late BP phase. Interestingly, previous studies showed that prefrontal-central interactions between the rIFG, the pre-SMA, and the primary motor cortex, subserving inhibitory aspects of motor control, occur in oscillatory bursts cycling at beta frequency.[43] A functional specialization in the beta-band might be therefore related to the proactive inhibition of action and even instrumental to a synergistic modulation of SMA and rIFG local activity in an accelerator/brake fashion. On the other hand, the functional meaning of beta-band activity can also be seen in light of sensorimotor and cognitive information maintenance within distributed networks.[44] Beta synchronization has been closely related to top-down processing[45,46] and might sub-serve the active maintenance of information within large-scale networks in the absence of external stimulation.[44,47] According to this view, beta-band connectivity might be related to proactive attentional control occurring while participants anticipate the appearance of visual stimuli that will inform them whether to release the inhibition or not.

Overall, our findings support the relevance of frequency-specific functional distributed networks, possibly playing a differential role in the processing of specific cognitive computations during early stages of movement preparation.[26,48,49] In this respect, functional connectivity patterns in the alpha, beta, and low-gamma bands between the left SMA, prefrontal and occipital regions change during BP time-course. Our study indicates that TMS-EEG can be an efficient tool to dissect and track functional reorganization in cortical connectivity occurring during action preparation, and provides unequivocal evidence of the involvement of complex inter-areal networks aiming at proactively ensuring a proper action unfolding. By supporting integration of functionally related information into unitary representations within distributed networks, pre-stimulus interactions between the premotor, prefrontal, and occipital regions might play a crucial role in the implementation of anticipatory cognitive computations, which can pave the way and bias the specification of the final action plan after the imperative signal is presented.[48–50]

The observed functional reorganization of inter-areal communication during preparatory stages of action might be beneficial for setting the sensorimotor system for readiness well before sensory events that require a motor response are presented, both in terms of effective and functional connectivity patterns. After stimulus perception and categorization, decision-making processes can take place and determine the appropriate output. Considering the interplay between inter-areal functional coupling and the regional activation of the motor system,[51] phase synchronization between cortical and subcortical brain structures may exert a modulatory action on brain regions activations, facilitating or suppressing the effective connectivity between two nodes of the same network, with critical consequences for the forthcoming selection of the appropriate motor output after stimulus presentation.

Our findings suggest that BP is not a mere result of an increased activation within premotor regions, but rather reflects a functional reorganization occurring within a distributed action preparation network that goes beyond the motor system, occurring during BP time-course. Changes in effective and functional connectivity may be driven by top-down mechanisms related to the anticipation of the forthcoming sensory event requiring a motor response, thus being functionally relevant to shape the activity of the motor regions during action preparation. This evidence supports further investigations in clinical conditions affecting motor and cognitive control of action, expanding the focus to non-motor regions functionally relevant to process the upcoming external stimuli and select the appropriate action pattern.

Limitations of study

The present experimental design did not allow us to directly assess the link between the TMS-EEG data and the behavioral performance: this step will be critical in future investigations to elucidate the functional role of the observed connectivity patterns during action execution.

STAR★METHODS

Detailed methods are provided in the online version of this paper and include the following:

- KEY RESOURCES TABLE
- RESOURCE AVAILABILITY
  - Lead contact
  - Materials availability
  - Data and code availability
- EXPERIMENTAL MODEL AND STUDY PARTICIPANT DETAILS
  - Human subjects
- METHOD DETAILS
  - Experimental procedures
  - TMS stimulation
  - EEG recording and pre-processing
- QUANTIFICATION AND STATISTICAL ANALYSIS
  - Behavioral data analysis
  - Electrophysiological data analysis

SUPPLEMENTAL INFORMATION

Supplemental information can be found online at https://doi.org/10.1016/j.isci.2023.107430.

ACKNOWLEDGMENTS

This work was supported by a grant from the University of Milano-Bicocca to A.P. (grant number 2018-ATE-0314).

AUTHOR CONTRIBUTIONS

Conceptualization, A.P., E.A., V.B., F.D.R., and L.J.R.L.; Methodology, A.P., E.A., V.B., F.D.R., and L.J.R.L.; Investigation, A.P., E.A., and V.B.; Visualization, A.P. and F.D.R.; Supervision, A.P., F.D.R., and L.J.R.L.; Writing—original draft: A.P., E.A., V.B., and F.D.R.; Writing—review & editing: A.P., E.A., V.B., F.D.R., and L.J.R.L.

DECLARATION OF INTERESTS

Authors declare that they have no competing interests.

INCLUSION AND DIVERSITY

We support inclusive, diverse, and equitable conduct of research.

Received: January 31, 2023
Revised: March 31, 2023
Accepted: July 17, 2023
Published: July 20, 2023

REFERENCES

1. Bestmann, S., and Duque, J. (2016). Transcranial Magnetic Stimulation: Decomposing the Processes Underlying Action Preparation. Neuroscientist *22*, 392–405. https://doi.org/10.1177/1073858415592594.

2. Neige, C., Rannaud Monany, D., and Lebon, F. (2021). Exploring cortico-cortical interactions during action preparation by means of dual-coil transcranial magnetic stimulation: A systematic review. Neurosci. Biobehav. Rev. *128*, 678–692. https://doi.org/10.1016/j.neubiorev.2021.07.018.

3. Di Russo, F., Berchicci, M., Bozzacchi, C., Perri, R.L., Pitzalis, S., and Spinelli, D. (2017). Beyond the "Bereitschaftspotential": Action preparation behind cognitive functions. Neurosci. Biobehav. Rev. *78*, 57–81. https://doi.org/10.1016/j.neubiorev.2017.04.019.

4. Colebatch, J.G. (2007). Bereitschaftspotential and movement-related potentials: Origin, significance, and application in disorders of human movement. Mov. Disord. *22*, 601–610. https://doi.org/10.1002/mds.21323.

5. Shibasaki, H., and Hallett, M. (2006). What is the Bereitschaftspotential? Clin. Neurophysiol. *117*, 2341–2356. https://doi.org/10.1016/j.clinph.2006.04.025.

6. Pedersen, J.R., Johannsen, P., Bak, C.K., Kofoed, B., Saermark, K., and Gjedde, A. (1998). Origin of human motor Readiness Field linked to left middle frontal gyrus by MEG and PET. Neuroimage *8*, 214–220. https://doi.org/10.1006/nimg.1998.0362.

7. Cunnington, R., Windischberger, C., Deecke, L., and Moser, E. (2003). The preparation and readiness for voluntary movement: A high-field event-related fMRI study of the Bereitschafts-BOLD response. Neuroimage

20, 404–412. https://doi.org/10.1016/S1053-8119(03)00291-X.

8. Ikeda, A., Lüders, H.O., Burgess, R.C., and Shibasaki, H. (1993). Movement-related potentials associated with single and repetitive movements recorded from human supplementary motor area. Electroencephalogr. Clin. Neurophysiol. *89*, 269–277. https://doi.org/10.1016/0168-5597(93)90106-Y.

9. Rektor, I. (2002). Scalp-recorded Bereitschaftspotential is the result of the activity of cortical and subcortical generators - A hypothesis. Clin. Neurophysiol. *113*, 1998–2005. https://doi.org/10.1016/S1388-2457(02)00286-9.

10. Rossi, S., Pasqualetti, P., Rossini, P.M., Feige, B., Ulivelli, M., Glocker, F.X., Battistini, N., Lucking, C.H., and Kristeva-Feige, R. (2000). Effects of repetitive transcranial magnetic stimulation on movement-related cortical activity humans. Cerebr. Cortex *10*, 802–808. https://doi.org/10.1093/cercor/10.8.802.

11. Ortu, E., Ruge, D., Deriu, F., and Rothwell, J.C. (2009). Theta Burst Stimulation over the human primary motor cortex modulates neural processes involved in movement preparation. Clin. Neurophysiol. *120*, 1195–1203. https://doi.org/10.1016/j.clinph.2009.04.001.

12. Lu, M.K., Arai, N., Tsai, C.H., and Ziemann, U. (2012). Movement related cortical potentials of cued versus self-initiated movements: Double dissociated modulation by dorsal premotor cortex versus supplementary motor area rTMS. Hum. Brain Mapp. *33*, 824–839. https://doi.org/10.1002/hbm.21248.

13. Cui, R.Q., and Deecke, L. (1999). High resolution DC-EEG analysis of the Bereitschaftspotential and post movement onset potentials accompanying uni- or bilateral voluntary finger movements. Brain Topogr. *11*, 233–249. https://doi.org/10.1023/A:1022237929908.

14. Ball, T., Schreiber, A., Feige, B., Wagner, M., Lücking, C.H., and Kristeva-Feige, R. (1999). The role of higher-order motor areas in voluntary movement as revealed by high-resolution EEG and fMRI. Neuroimage *10*, 682–694. https://doi.org/10.1006/nimg.1999.0507.

15. Cui, R.Q., Huter, D., Lang, W., and Deecke, L. (1999). Neuroimage of voluntary movement: Topography of the Bereitschaftspotential, a 64-channel DC current source density study. Neuroimage *9*, 124–134. https://doi.org/10.1006/nimg.1998.0388.

16. Casarotto, S., Romero Lauro, L.J., Bellina, V., Casali, A.G., Rosanova, M., Pigorini, A., Defendi, S., Mariotti, M., and Massimini, M. (2010). EEG responses to TMS are sensitive to changes in the perturbation parameters and repeatable over time. PLoS One *5*, e10281. https://doi.org/10.1371/journal.pone.0010281.

17. Miniussi, C., and Thut, G. (2010). Combining TMS and EEG offers new prospects in cognitive neuroscience. Brain Topogr. *22*, 249–256. https://doi.org/10.1007/s10548-009-0083-8.

18. Massimini, M., Ferrarelli, F., Huber, R., Esser, S.K., Singh, H., and Tononi, G. (2005). Neuroscience: Breakdown of cortical effective connectivity during sleep. Science *309*, 2228–2232. https://doi.org/10.1126/science.1117256.

19. Pisoni, A., Romero Lauro, L.J., Vergallito, A., Maddaluno, O., and Bolognini, N. (2018). Cortical dynamics underpinning the self-other distinction of touch: A TMS-EEG study. Neuroimage *178*, 475–484. https://doi.org/10.1016/j.neuroimage.2018.05.078.

20. Di Russo, F., Berchicci, M., Bianco, V., Rl, P., Pitzalis, S., Quinzi, F., and Spinelli, D. (2019). Normative event-related potentials from sensory and cognitive tasks reveal occipital and frontal activities prior and following visual events. Neuroimage *196*, 173–187. https://doi.org/10.1016/j.neuroimage.2019.04.033.

21. Di Russo, F., Lucci, G., Sulpizio, V., Berchicci, M., Spinelli, D., Pitzalis, S., and Galati, G. (2016). Spatiotemporal brain mapping during preparation, perception, and action. Neuroimage *126*, 1–14. https://doi.org/10.1016/j.neuroimage.2015.11.036.

22. Massimini, M., Ferrarelli, F., Huber, R., Esser, S.K., Singh, H., and Tononi, G. (2005). Breakdown of cortical effective connectivity during sleep. Science *309*, 2228–2232. https://doi.org/10.1126/science.1117256.

23. Vinck, M., Oostenveld, R., Van Wingerden, M., Battaglia, F., and Pennartz, C.M.A. (2011). An improved index of phase-synchronization for electrophysiological data in the presence of volume-conduction, noise and sample-size bias. Neuroimage *55*, 1548–1565. https://doi.org/10.1016/j.neuroimage.2011.01.055.

24. Aron, A.R. (2011). From reactive to proactive and selective control: Developing a richer model for stopping inappropriate responses. Biol. Psychiatr. *69*, e55–e68. https://doi.org/10.1016/j.biopsych.2010.07.024.

25. Bianco, V., Berchicci, M., Perri, R.L., Spinelli, D., and Di Russo, F. (2017). The proactive self-control of actions: Time-course of underlying brain activities. Neuroimage *156*, 388–393. https://doi.org/10.1016/j.neuroimage.2017.05.043.

26. Von Stein, A., and Sarnthein, J. (2000). Different frequencies for different scales of cortical integration: From local gamma to long range alpha/theta synchronization. Int. J. Psychophysiol. *38*, 301–313. https://doi.org/10.1016/S0167-8760(00)00172-0.

27. Lee, K.H., Williams, L.M., Breakspear, M., and Gordon, E. (2003). Synchronous Gamma activity: A review and contribution to an integrative neuroscience model of schizophrenia. Brain Res. Rev. *41*, 57–78. https://doi.org/10.1016/S0165-0173(02)00220-5.

28. Engel, A.K., and Singer, W. (2001). Temporal binding and the neural correlates of sensory awareness. Trends Cognit. Sci. *5*, 16–25. https://doi.org/10.1016/S1364-6613(00)01568-0.

29. Fries, P. (2009). Neuronal gamma-band synchronization as a fundamental process in cortical computation. Annu. Rev. Neurosci. *32*, 209–224. https://doi.org/10.1146/annurev.neuro.051508.135603.

30. Fries, P. (2015). Rhythms for Cognition: Communication through Coherence. Neuron *88*, 220–235. https://doi.org/10.1016/j.neuron.2015.09.034.

31. Joundi, R.A., Jenkinson, N., Brittain, J.S., Aziz, T.Z., and Brown, P. (2012). Driving oscillatory activity in the human cortex enhances motor performance. Curr. Biol. *22*, 403–407. https://doi.org/10.1016/j.cub.2012.01.024.

32. Brown, P. (2003). Oscillatory nature of human basal ganglia activity: Relationship to the pathophysiology of parkinson's disease. Mov. Disord. *18*, 357–363. https://doi.org/10.1002/mds.10358.

33. Schoffelen, J.M., Oostenveld, R., and Fries, P. (2005). Neuronal coherence as a mechanism of effective corticospinal interaction. Science *308*, 111–113. https://doi.org/10.1126/science.1107027.

34. Picard, N., and Strick, P.L. (1996). Motor areas of the medial wall: A review of their location and functional activation. Cerebr. Cortex *6*, 342–353. https://doi.org/10.1093/cercor/6.3.342.

35. Shima, K., and Tanji, J. (1998). Role for cingulate motor area cells in voluntary movement selection based on reward. Science *282*, 1335–1338. https://doi.org/10.1126/science.282.5392.1335.

36. Swick, D., and Turken, A.U. (2002). Dissociation between conflict detection and error monitoring in the human anterior cingulate cortex. Proc. Natl. Acad. Sci. USA *99*, 16354–16359. https://doi.org/10.1073/pnas.252521499.

37. Waszak, F., Cardoso-Leite, P., and Hughes, G. (2012). Action effect anticipation: Neurophysiological basis and functional consequences. Neurosci. Biobehav. Rev. *36*, 943–959. https://doi.org/10.1016/j.neubiorev.2011.11.004.

38. Palva, S., and Palva, J.M. (2011). Functional roles of alpha-band phase synchronization in local and large-scale cortical networks. Front. Psychol. *2*, 204–215. https://doi.org/10.3389/fpsyg.2011.00204.

39. Palva, S., and Palva, J.M. (2007). New vistas for α-frequency band oscillations. Trends Neurosci. *30*, 150–158. https://doi.org/10.1016/j.tins.2007.02.001.

40. Lobier, M., Palva, J.M., and Palva, S. (2018). High-alpha band synchronization across frontal, parietal and visual cortex mediates behavioral and neuronal effects of visuospatial attention. Neuroimage *165*, 222–237. https://doi.org/10.1016/j.neuroimage.2017.10.044.

41. Capotosto, P., Babiloni, C., Romani, G.L., and Corbetta, M. (2009). Frontoparietal cortex controls spatial attention through modulation of anticipatory alpha rhythms. J. Neurosci. *29*,

5863–5872. https://doi.org/10.1523/JNEUROSCI.0539-09.2009.

42. Sauseng, P., Feldheim, J.F., Freunberger, R., and Hummel, F.C. (2011). Right prefrontalTMS disrupts interregional anticipatory EEG alpha activity during shifting of visuospatial attention. Front. Psychol. *2*, 241. https://doi.org/10.3389/fpsyg.2011.00241.

43. Picazio, S., Veniero, D., Ponzo, V., Caltagirone, C., Gross, J., Thut, G., and Koch, G. (2014). Prefrontal control over motor cortex cycles at beta frequency during movement inhibition. Curr. Biol. *24*, 2940–2945. https://doi.org/10.1016/j.cub.2014.10.043.

44. Engel, A.K., and Fries, P. (2010). Beta-band oscillations-signalling the status quo? Curr. Opin. Neurobiol. *20*, 156–165. https://doi.org/10.1016/j.conb.2010.02.015.

45. Gross, J., Schmitz, F., Schnitzler, I., Kessler, K., Shapiro, K., Hommel, B., and Schnitzler, A. (2004). Modulation of long-range neural synchrony reflects temporal limitations of visual attention in humans. Proc. Natl. Acad. Sci. USA *101*, 13050–13055. https://doi.org/10.1073/pnas.0404944101.

46. Buschman, T.J., and Miller, E.K. (2007). Top-Down Versus Bottom-Up Control of Attention in the Prefrontal and Posterior Parietal Cortices. Science *315*, 1860–1862.

47. Siegel, M., Donner, T.H., and Engel, A.K. (2012). Spectral fingerprints of large-scale neuronal interactions. Nat. Rev. Neurosci. *13*, 121–134. https://doi.org/10.1038/nrn3137.

48. Buzsáki, G., and Draguhn, A. (2004). Neuronal Oscillations in Cortical Networks. Science *304*, 1926–1929.

49. Kim, K., Kim, J.S., and Chung, C.K. (2017). Increased gamma connectivity in the human prefrontal cortex during the bereitschaftspotential. Front. Hum. Neurosci. *11*, 180–189. https://doi.org/10.3389/fnhum.2017.00180.

50. Von Stein, A., Chiang, C., and König, P. (2000). Top-down processing mediated by interareal synchronization. Proc. Natl. Acad. Sci. USA *97*, 14748–14753. https://doi.org/10.1073/pnas.97.26.14748.

51. Gerloff, C., Richard, J., Hadley, J., Schulman, A.E., Honda, M., and Hallett, M. (1998). Functional coupling and regional activation of human cortical motor areas during simple, internally paced and externally paced finger movements. Brain *121*, 1513–1531. https://doi.org/10.1093/brain/121.8.1513.

52. Delorme, A., and Makeig, S. (2004). EEGLAB: an open source toolbox for analysis of single-trial EEG dynamics including independent component analysis. J. Neurosci. Methods *134*, 9–21. https://doi.org/10.1016/j.jneumeth.2003.10.009.

53. Oostenveld, R., Fries, P., Maris, E., and Schoffelen, J.M. (2011). FieldTrip: Open source software for advanced analysis of MEG, EEG, and invasive electrophysiological data. Comput. Intell. Neurosci. *2011*, 156869. https://doi.org/10.1155/2011/156869.

54. R Core Team (2020). R: A Language and Environment for Statistical Computing.

55. Faul, F., Erdfelder, E., Buchner, A., and Lang, A.-G. (2009). Statistical power analyses using G*Power 3.1: Tests for correlation and regression analyses. Behav. Res. Methods *41*, 1149–1160.

56. Rossi, S., Antal, A., Bestmann, S., Bikson, M., Brewer, C., Brockmöller, J., Carpenter, L.L., Cincotta, M., Chen, R., Daskalakis, J.D., et al. (2021). Safety and recommendations for TMS use in healthy subjects and patient populations, with updates on training, ethical and regulatory issues: Expert Guidelines. Clin. Neurophysiol. *132*, 269–306. https://doi.org/10.1016/j.clinph.2020.10.003.

57. Virtanen, J., Ruohonen, J., Näätänen, R., and Ilmoniemi, R.J. (1999). Instrumentation for the measurement of electric brain responses to transcranial magnetic stimulation. Med. Biol. Eng. Comput. *37*, 322–326. https://doi.org/10.1007/BF02513307.

58. Romero Lauro, L.J., Rosanova, M., Mattavelli, G., Convento, S., Pisoni, A., Opitz, A., Bolognini, N., and Vallar, G. (2014). TDCS increases cortical excitability: Direct evidence from TMS-EEG. Cortex *58*, 99–111. https://doi.org/10.1016/j.cortex.2014.05.003.

59. Romero Lauro, L.J., Pisoni, A., Rosanova, M., Casarotto, S., Mattavelli, G., Bolognini, N., and Vallar, G. (2016). Localizing the effects of anodal tDCS at the level of cortical sources: A Reply to Bailey et al., 2015. Cortex *74*, 323–328. https://doi.org/10.1016/j.cortex.2015.04.023.

60. Bates, D., Maechler, M., Bolker, B., Walker, S., Haubo, R., Christensen, B., Singmann, H., Dai, B., Scheipl, F., Grothendieck, G., et al. (2018). Package "lme4.".

61. Fuchs, M., Kastner, J., Wagner, M., Hawes, S., and Ebersole, J.S. (2002). A standardized boundary element method volume conductor model integral equation using analytically integrated elements. Clin. Neurophysiol. *113*, 702–712.

62. Vorwerk, J., Cho, J.H., Rampp, S., Hamer, H., Knösche, T.R., and Wolters, C.H. (2014). A guideline for head volume conductor modeling in EEG and MEG. Neuroimage *100*, 590–607. https://doi.org/10.1016/j.neuroimage.2014.06.040.

63. Fischl, B. (2012). Neuroimage *62*, 774–781. https://doi.org/10.1016/j.neuroimage.2012.01.021.

64. Mahjoory, K., Nikulin, V.V., Botrel, L., Linkenkaer-Hansen, K., Fato, M.M., and Haufe, S. (2017). Consistency of EEG source localization and connectivity estimates. Neuroimage *152*, 590–601. https://doi.org/10.1016/j.neuroimage.2017.02.076.

65. Popov, T., Oostenveld, R., and Schoffelen, J.M. (2018). FieldTrip Made Easy: An Analysis Protocol for Group Analysis of the Auditory Steady State Brain Response in Time, Frequency, and Space. Front. Neurosci. *12*, 711. https://doi.org/10.3389/fnins.2018.00711.

66. Pascual-Marqui, R.D., Lehmann, D., Koukkou, M., Kochi, K., Anderer, P., Saletu, B., Tanaka, H., Hirata, K., John, E.R., Prichep, L., et al. (2011). Assessing interactions in the brain with exact low-resolution electromagnetic tomography. Philos. Trans. A Math. Phys. Eng. Sci. *369*, 3768–3784. https://doi.org/10.1098/rsta.2011.0081.

67. Tzourio-Mazoyer, N., Landeau, B., Papathanassiou, D., Crivello, F., Etard, O., Delcroix, N., Mazoyer, B., and Joliot, M. (2002). Automated Anatomical Labeling of Activations in SPM Using a Macroscopic Anatomical Parcellation of the MNI MRI Single-Subject Brain. Neuroimage *15*, 273–289. https://doi.org/10.1006/nimg.2001.0978.

68. Hillebrand, A., Barnes, G.R., Bosboom, J.L., Berendse, H.W., and Stam, C.J. (2012). Frequency-dependent functional connectivity within resting-state networks: An atlas-based MEG beamformer solution. Neuroimage *59*, 3909–3921. https://doi.org/10.1016/j.neuroimage.2011.11.005.

69. Maris, E., and Oostenveld, R. (2007). Nonparametric statistical testing of EEG- and MEG-data. J. Neurosci. Methods *164*, 177–190. https://doi.org/10.1016/j.jneumeth.2007.03.024.

STAR★METHODS

KEY RESOURCES TABLE

REAGENT or RESOURCE	SOURCE	IDENTIFIER
Software and algorithms		
MATLAB	MathWorks	R2019a
EEGLAB	Delorme & Makeig, 2004,[52]	https://eeglab.org V13.5.4b
Fieldtrip Toolbox	Oostenveld et al., 2011,[53]	https://www.fieldtriptoolbox.org V20200115
E-Prime 2	Psychology Software Tools Inc.	https://pstnet.com/products/e-prime-legacy-versions/ V2.1
R-Studio	RStudio Team (2020),[54]	http://www.rstudio.com/
Custom code	This paper	https://osf.io/ha7es/?view_only=223089c22d4c47b0936e475d421af6c5
G*Power 3.1	Faul et al., 2009[55]	https://www.psychologie.hhu.de/arbeitsgruppen/allgemeine-psychologie-und-arbeitspsychologie/gpower
Deposited data		
Raw and analyzed data	This paper	https://osf.io/ha7es/?view_only=223089c22d4c47b0936e475d421af6c5
Other		
Eximia TMS-compatible EEG amplifier	Nexstim™, Helsinki, Finland	N/A
Eximia™ TMS stimulator	Nexstim™, Helsinki, Finland	https://www.nexstim.com/healthcare-professionals/nbs-system
BiPulse 70-mm figure-of-eight coil	Nexstim™, Helsinki, Finland	N/A
Navigated Brain Stimulation (NBS) system	Nexstim™, Helsinki, Finland	https://www.nexstim.com/healthcare-professionals/technology
EASYCAP 60-channels HD-EEG cap	Easycap GmbH, Munich, Germany	BC-TMS-64-X11-SCMW-56

RESOURCE AVAILABILITY

Lead contact

Further information and requests for resources should be directed to and will be fulfilled by the lead contact, Prof. Alberto Pisoni (alberto.pisoni@unimib.it).

Materials availability

This study did not generate new materials.

Data and code availability

- .mat TMS-EEG data are deposited at Open Science Framework Repository and will be available as of the date of publication. In addition, summary statistics describing these data and processed datasets derived from these data have been deposited at Open Science Framework Repository and are publicly available as of the date of publication. The accession numbers are listed in the key resources table.
- All original code is deposited at Open Science Framework Repository and will be publicly available as of the date of publication. DOI/URLs are listed in the key resources table.
- Any additional information required to reanalyze the data reported in this paper is available from the lead contact upon request.

EXPERIMENTAL MODEL AND STUDY PARTICIPANT DETAILS

Human subjects

Fourteen healthy, right-handed volunteers (8 females, mean (±standard deviation, SD) age = 24.3 ±2.2 years) took part in this study. The study's sample size was estimated by means of an a-priori power analysis using the software G*Power 3.1. The analysis was based on a 2x2 within-factors repeated measures ANOVA design (Factors: 'TMS SOA', 2 levels; 'TMS target', 2 levels), with a medium effect size=0.5, alpha=0.05, and power=0.90.

All participants belonged to the same experimental group and underwent the same procedures. They all had a normal or corrected-to-normal vision and no history of neurological, psychiatric, or other relevant medical condition and were naïve to the experimental procedures. Each participant completed a safety screening questionnaire to exclude the presence of contraindication to TMS following the current TMS safety guidelines[56] and gave informed written consent prior to their participation in the study. The study was performed in the TMS-EEG laboratory of the University of Milano-Bicocca in accordance with the Declaration of Helsinki and the approval of the local Ethics Committee.

METHOD DETAILS

Experimental procedures

Participants sat comfortably at room temperature in a semi-reclined armchair in front of a 20" computer screen at a distance of 114 cm, with their arms on the armrests and their right hand positioned on a PC mouse, allowing them to press a button with their right index finger.

The experimental conditions were tested in a four-block recording session performed on one day. In each block, participants were asked to perform an uncued, visual Go/No-Go task during the TMS-EEG recording. Each trial started with a fixation point, a yellow dot displayed at the centre of the screen on a black background, which remained present on the screen for the entire trial. Then, in a random jittering interval ranging from 2900ms to 3900ms according to trial type, a TMS pulse was delivered. After the corresponding SOA (i.e., 300ms or 700ms) one of four different visual stimuli, made by four squared configurations with vertical and horizontal bars (4°x4° of visual angle, Figure 1), was randomly presented in focal vision for 250ms, with equal probability (p=0.25). Two configurations were defined as targets, thus requiring the participants to produce the motor response (i.e., *Go* trials, p=0.5), and two as non-targets and they were associated with the instruction to withhold the response (i.e., *No-Go* trials, p=0.5). Visual stimulus SOA was jittered to reduce anticipatory responses and to avoid ERP overlap with the previous trial. Then, participants' responses were collected (max 1500ms). In total, 60 trials for each experimental condition were collected (Go/No-Go trials * 2 SOAs and * 2 cortical targets); 60 additional trials were collected in each recording block, in which we delivered TMS over the left SMA or V2 while participants were at rest, staring at the fixation point on the screen (see supplemental information). 120 trials were additionally recorded while participants performed the Go/No-Go task without TMS, for a total of 720 trials, divided in 180 trials blocks. The duration of each block was approximately 10 minutes, and their order was counterbalanced between subjects.

TMS pulses were delivered at two alternative target sites (2 blocks each), following MNI coordinates derived from a previous fMRI study[21]: the left SMA (x=-4, y=17, z=45) a potential generator of the BP, and the left extrastriate visual cortex (x=-21, y=-98, z=5), unrelated to BP origins, but still a potential node of the action preparation network, especially when visual cues are concerned.[20] Before the experimental session, a short practice familiarized participants with the stimuli and the task.

Trials randomization, TMS and visual stimuli timing, and behavioural data recording (i.e., response times, RT, and accuracy) were under computer control (E-Prime, Psychology Software Tools Inc.), as well as TMS and EEG trigger delivery.

TMS stimulation

Single-pulse biphasic TMS was delivered with an Eximia™ TMS stimulator (Nexstim™, Helsinki, Finland) using a biphasic focal figure-of-eight 70mm coil. The stimulation target sites were localized on normalized individual high-resolution (1mm^3) MRI images at the selected MNI coordinates. The location of the two stimulation targets was identified for each participant using a Navigated Brain Stimulation (NBS) system

(Nexstim™, Helsinki, Finland) based on infrared-based frameless stereotaxy, allowing also an accurate monitoring of the position and orientation of the coil and an online estimation of the distribution and intensity (V/m) of the intracranial electric field induced by the TMS. TMS intensity was preliminarily adjusted for each participant and cortical target before the experiment, to ensure an early cortical response of at least 6μV, as assessed online in a short recording session before the experimental blocks. The mean intensity of the electric field induced by TMS was 98.57 V/m (SD=±16.55) for the left SMA, and 94.86 V/m (SD=±17.18) for the left extrastriate region, corresponding to a mean intensity – expressed as percentage of the maximal stimulator output (MSO) – of 63.21% (SD=±2.49) for the SMA, and 63.21% (SD=±2.49) for the extrastriate region.

EEG recording and pre-processing

EEG data were continuously acquired from 60 channels using a sample-and-hold[57] TMS-compatible system (Nexstim™, Helsinki, Finland). Two electrodes were placed over the forehead as ground. Two additional electro-oculographic (EOG) channels were placed near the eyes and used to monitor ocular artifacts due to eye movements and blinking. Noise-masking was performed by continuously playing into earplugs an audio track created by shuffling TMS discharge noise, to prevent the emergence of auditory evoked potentials (as in[19,58,59]). Electrodes' impedance was kept below 5 kΩ. EEG signals were acquired with a sampling rate of 1450 Hz.

Data pre-processing was carried out using MATLAB R2019a (Mathworks, Natick, MA, USA). First, EEG data was down-sampled to 725 Hz. Continuous signal was segmented in epochs starting 1000 ms pre- and ending 1000 ms post-TMS pulse. A band-pass filter between 0.2 and 80 Hz and a 50 Hz notch filter were applied to the selected epochs. Single trials with excessive artifacts were rejected by visual inspection. Bad channels were excluded and then interpolated using a spherical interpolation function included in EEGLAB.[52]

TMS-evoked potentials (TEPs) were computed by averaging artifact-free trials, re-referenced using an average reference, and baseline-corrected between -900 and -700 ms before TMS pulse. Independent Component Analysis (INFOMAX ICA) was performed to remove residual artifacts due to TMS pulse, muscle contraction, or eye movements. We removed M=11.6, SD=4.8 components for SMA TMS data, and M=13.2, SD=4.2 components for V2 TMS data. The number of components removed does not statistically differ between the two conditions: t(27)=-1.45, p=0.16.

QUANTIFICATION AND STATISTICAL ANALYSIS

Behavioral data analysis

Statistical analyses were carried out using RStudio.[54]

RTs of correct go trials were compared across stimulation conditions through a series of Linear Mixed Models, using the ''lmer'' function in the R package "lme4" (version 1.1-5,[60]). As fixed effect TMS target (2 levels: SMA and V2) and SOA (2 levels: -700ms and -300ms) and their interaction were considered as factorial predictors, and the order of trials as a covariate to control for learning effects during task execution. By-subjects random intercept was included to account for inter-individual differences. Concerning accuracy, we compared the accuracy data across conditions using the generalized mixed models for binomially distributed variables with the ''glmer'' procedure implemented in the ''lme4'' R package, using the binomial link function. As for RTs analysis, we first considered as fixed effects TMS target, SOA as predictors, as well as Trial Type (2 levels: Go vs. No-Go) and their interaction, and the order of the trials as a covariate. By-subjects random intercepts were included to account for inter-individual differences.

Electrophysiological data analysis

As the aim of the study was to investigate the cortical dynamics underlying action preparation, all the analyses focused exclusively on the pre-stimulus time window. Therefore, the distinction between *Go* and *No-Go* Trials was not taken into account.[20]

First, to confirm the BP occurrence in the present paradigm, for the No-TMS block the ERPs associated with the visual stimulus onset were calculated. For this purpose, EEG was segmented in 1500 ms windows beginning 1200 ms before visual stimulus onset and ending 300 ms after.

Then, effective and functional connectivity were computed at the source level. The forward model was created starting from a Boundary Element Model (BEM) obtained segmenting a subject MRI into five standard tissues (Gray and white matters, CSF, Skull, and Scalp). The head model was then computed assigning standard conductivity values for the scalp, skull, and brain compartments.[61,62] Source space was defined performing a cortical reconstruction and volumetric segmentation of the grey matter with the Freesurfer image analysis suite,[63] down-sampled to 8194 cortical sources, and realigned to the head model space. Finally, individual lead-field matrices were computed by aligning this forward model with the individual electrode positions, which were recorded during each TMS-EEG session. Source reconstruction of the EEG time-series was conducted with the eLORETA method implemented in Fieldtrip[64–66] for solving the inverse modelling. Source signals were then segmented in 88 regions of interest (ROIs) according to the AAL atlas.[67] The computed source time-series were then averaged to index each ROI source activation[68] and effective and functional connectivity analyses were performed using the Fieldtrip toolbox.[53] Specifically, to track changes in cortical excitability occurring during the BP time-course, we compared the amplitude of cortical activations at the two TMS SOAs (i.e., -700 ms vs -300 ms) within each stimulation site (i.e., left SMA and extrastriate regions). The comparison between the two SOAs was also performed for other regions involved in the motor preparation/execution network: the left/right SMA, primary motor, premotor cortex, secondary visual regions and the right inferior frontal gyrus.[21] Within each cluster, cortical activation amplitude time-course was compared using a dependent sample t-test with a nonparametric cluster-based permutation approach.[69] In the present study, for each comparison, we performed 10000 permutations on the time window between 0 and 250 ms post-TMS and used a permutation-significance threshold of $p=0.05$. Using the same approach, activations induced by extrastriate TMS were compared in the same cortical parcels. Time-frequency analysis was perfomed with a multitaper method as implemented in Fieldtrip.[19,53] Then, the debiased Wheighted Phase Lag Index (WPLI,[23]) was computed between the left SMA and the other brain parcels for alpha (8-12 Hz), beta (13-30 Hz), low gamma (31-40 Hz) bands for the two TMS SOAs, with a particular interest for beta and gamma frequency, as suggested by Kim et al.[49] This analysis was also performed on a surrogate dataset created by shuffling the phase of the source reconstructed time series for each experimental condition. Surrogates were created starting from real data, by shuffling the phase using the "phaseran" Matlab function, to keep oscillatory power comparable to the original data but disrupting potential phase interactions (as in Pisoni et al., 2018). For each participant and each condition, thus, a surrogate dataset was created and entered the described connectivity analysis pipeline. To reduce the risk that spurious connectivity could be included in our results, real data were compared with the surrogate ones computing a t-test performed on each connectivity pair (87, SMA with the other 87 brain parcels) and corrected for multiple comparisons based on 2000 permutation approach, implemented in MATLAB, with a significance level of $p=0.01$.[19] Surviving connections were plotted to highlight the resulting FC between the left SMA and the other parcels.